Stoichiometry control and automated growth of alkali antimonide photocathode films by molecular beam deposition

Pavlenko, Vitaly
Smedley, John Morgan
Scheinker, Alexander
Fleming, Ryan Lee
Alexander, Anna Marie
Hoffbauer, Mark Arles
Moody, Nathan Andrew

To be published in: Applied Physics Letters

DOI to publisher's version: 10.1063/5.0080948

Permalink to record:
http://permalink.lanl.gov/object/view?what=info:lanl-repo/lareport/LA-UR-21-30432

Stoichiometry control and automated growth of alkali antimonide photocathode films by molecular beam deposition

Vitaly Pavlenko[a], John Smedley, Alexander Scheinker, Ryan L. Fleming, Anna Alexander, Mark A. Hoffbauer, and Nathan A. Moody

Los Alamos National Laboratory (LANL), P.O. Box 1663, Los Alamos, New Mexico 87545, USA

[a] Author to whom correspondence should be addressed: pavlenko@lanl.gov

ABSTRACT We report on a method of photoemissive film growth that controls stoichiometry in real time. We show that stoichiometry control using a feedback loop is possible because (a) photoemissive properties exhibit a distinct dependence on the stoichiometric composition, and (b) stoichiometric composition strongly depends on the ratio of the incident fluxes. The reported results were obtained on Cs_3Sb but are expected to be relevant to other alkali antimonides and tellurides.

Alkali antimonide photocathode films such as Cs_3Sb and K_2CsSb are likely candidates for the next generation electron sources with high beam brightness [1]. However, while exciting results of material engineering have been accomplished in user-facilities [2-4], the state of the art for injector growth systems is represented by nanocrystalline films, whose physical and chemical roughness does not allow to approach the thermal limit of the mean transverse energy of emitted electrons [5]. Significant progress is needed in the growth technology in order to fabricate near atomically smooth single crystalline alkali antimonide thin films, and this technology needs to be transferable to cathodes that can be used in injectors. The study presented in this Letter addresses the issue of stoichiometry control, a pre-requisite for elaborate growth techniques such as molecular beam epitaxy (MBE), and does not rely on expensive and/or time-consuming techniques involving Kelvin probe force microscopy (KPFM) [5], scanning tunneling microscopy (STM) [4] or synchrotrons [2, 3] to achieve it.

Strong effect of alkali antimonides' stoichiometry on the quantum efficiency (QE) was discovered more than 50 years ago in the context of the studies of polarity of conductivity, see Chapter 6 in Ref. [6]. It was established experimentally that maximum photoemission is attained not at 3:1 Sb-to-alkali atomic ratio but with a small (a few percent [7, 8]) stoichiometric offset instead. The peak of photoemission was found to coincide with the stable state of the compound, the one that is achieved when a film with excess alkali content eventually loses it into vacuum [6]. In this Letter, we will refer to such slightly off-stoichiometric composition that corresponds to maximum photoemission as optimum stoichiometry.

The studies mentioned above were conducted on the films obtained by sequential deposition method when a film undergoes extremely wide changes in stoichiometry, starting with 100% antimony, then significantly alkali-rich, finally arriving at the optimum [6, 9]. The significance of stoichiometry control is greatly amplified for the case of molecular beam deposition, when the goal is to slowly grow a uniform film that was also shown to be significantly smoother [2, 10]. To differentiate from sequential deposition, molecular beam deposition of alkali antimonides is often dubbed as co-deposition [4, 10, 11] or co-evaporation [2]. The fact that the ratio of incident fluxes has a strong effect on the QE a growing alkali antimonide film has been reliably established experimentally [4, 11-14]. Thus, within a fairly wide range in the vicinity of optimum stoichiometry the ratio of incident fluxes affects the stoichiometric composition, hence dynamically adjusting the ratio creates a tool to control the stoichiometry.

Adjusting the ratio of incident fluxes during the growth is indeed a common practice in the field to achieve higher QE, with some reports claiming that QE maximization can actually be accomplished [4, 13]. Given the absence of details on the flux adjustment procedures, we are led to believe that those are manual and largely intuitive actions that are somewhat successful at attaining higher QE at the end of the growth, but are not truly maximizing instantaneous QE in real time. In fact, it would be impossible to implement a QE maximization scheme, because QE of the film is also a function of its thickness [6, 15]. One could arguably normalize QE by the film's thickness first or attempt to maximize the rate of QE increase vs time. Although not impossible in principle, practical realization of such schemes would introduce another level of ambiguity and complexity, making it prone to lags and instabilities.

Sample to sample variation of alkali antimonide films QE is rarely mentioned, but whenever reported is very large [4, 13,14] – a ratio of two or more between the best and the worst sample in a series, and so is the variation of stoichiometric composition [14] and of the ratio of fluxes [4, 13] – several tens of percent. It is therefore reasonable to consider poor stoichiometry control as a significant, if not dominant, factor in unsatisfactory reproducibility of alkali antimonide film growth experiments.

The study reported in this Letter was conducted in a UHV molecular beam deposition system [16]. Stable and relatively agile pre-calibrated elemental sources were used to obtain the necessary accuracy of flux control (of the order of 1%). The fluxes were directed at about 15 degrees with respect to sample substrate normal, with flux non-uniformity across 1 cm substrate estimated to be better than 10%. Laser diode modules attenuated to deliver ~100 μW in a ~1 mm^2 spot were used for intermittent photo-excitation of the samples with a moderate sampling rate (~0.1 Hz), synchronized with the photocurrent measurements. A bias of approximately 100 V was applied to an anode ring placed at 2-3 cm in front of the sample; collected photocurrent was measured by a picoammeter. Commercial Si substrates were cleaned at 600^{o}C in UHV for a few hours prior to depositions.

In order to establish true stoichiometry control, one first needs to find a parameter that (i) is fundamentally related to stoichiometry, (ii) can be measured *in situ* as the film is growing, and (iii) is film thickness-independent [12]. We provide here an experimental demonstration that such parameter can be identified, owing to the fact that not only QE of an alkali antimonide film strongly depends on the stoichiometry in a wide range of wavelengths, but the shape of the spectral response curve also changes, see Fig. 1. We chose to track the ratio of QEs measured well above the photoemission threshold (at 405 nm, QE_{405nm}) and slightly above the threshold (at 532 nm, QE_{532nm}). It is likely that the change of the ratio is related to the shift of photoemission threshold of a few tens of meV [12], but because of uncertainty in the determination of the threshold value further studies are required to make a stronger statement. The growth (Fig. 1) is started in Cs-rich mode, then as Cs flux is slowly ramped down optimum growth condition is achieved at some point with subsequent transition into Sb-rich mode. Because of a relatively high substrate temperature (roughly estimated at 80^{o}C [17]) and slow growth rate (about 0.03 Å/s) the excess Cs atoms are expected to have enough time to diffuse through the bulk of the film towards the top, hence during the experiment largely the whole film undergoes transition from slightly Cs-rich to slightly Sb-rich, not just its top layer. Nonetheless, in a dynamic equilibrium some non-uniformity remains, therefore the dependence in Fig. 1 should be interpreted semi-quantitatively as follows. Because the ratio of fluxes changes approximately linearly vs time, time axis effectively represents stoichiometry (note that we limited ourselves to defining the fluxes ratio in arbitrary units because of calibration uncertainties, however the atomic ratio is indeed close to 3:1, indicating that the effective rejection rate for Cs is low). Thus, a well-defined dependence with an asymmetric minimum of QE_{405nm}/QE_{532nm} vs stoichiometric composition exists (Fig. 1), making QE_{405nm}/QE_{532nm} a parameter that satisfies all three requirements mentioned above. In light of the dependence of the photoemissive properties on the stoichiometric compositions (Fig. 1), pronounced oscillations of the QEs and QE_{405nm}/QE_{532nm} observed in response to a modulated Cs/Sb flux ratio in [12] can be largely attributed to the periodic variations of the film's stoichiometry, while in Cs-rich growth mode; the fact that the oscillations of the QEs are essentially in phase with each other but out of phase with respect to the QE_{405nm}/QE_{532nm} oscillations suggests that position of the minimum of QE_{405nm}/QE_{532nm} is close to the optimum stoichiometry in terms of maximum photoemission (dominated by QE well above the threshold) in Sommer's experiments, Chapter 6 in [6]. The ratio of QEs QE_{405nm}/QE_{532nm} can enable real-time control of alkali antimonide stoichiometric composition if used as an optimization parameter in a feedback loop. In an ideal situation, one would probably want to target the very minimum value of the parameter. Practically, we have to deal with the limitations of our instrumentation, so we chose to confine ourselves within the Cs-rich range of stoichiometry (to the left from the minimum in Fig. 1). Within that range the correlation between QE_{405nm}/QE_{532nm} and fluxes ratio is very strong and always positive, making it possible to employ simple yet robust feedback loop such as proportional–integral–derivative (PID) controller. Targeting the values of QE_{405nm}/QE_{532nm} of about 2 should result in production of a few percent Cs-rich film. Coincidentally, producing a slightly Cs-rich rather than a slightly Sb-rich film is likely beneficial since excess alkali metal will be naturally removed from the film after the growth [6].

An example of Cs_3Sb growth controlled by a PID loop targeting the value of optimization parameter QE_{405nm}/QE_{532nm} of 2.2 by adjusting Sb flux is shown in Fig. 2. Prior to the experiment, the PID gains for an approach with some overshoot were found using Ziegler–Nichols method. The values of PID gains are highly system-dependent, therefore without universal significance. Tuning the PID loop differently would certainly affect the approach to target, as would a different algorithm type. We confirmed that an extremum seeking algorithm [18] set to minimize the value of $\left|\frac{QE_{405nm}}{QE_{532nm}} - Target\right|$ can be used instead of a PID controller. After initial settling process, the algorithm locks on the target at about 3000 s. Overall, the evolution of QEs proceeds as expected for a uniform film – approximately linear growth in the beginning of the cycle followed by saturation. Noticeable dips on QE_{405nm} and, especially, QE_{532nm} dependences between approximately 1500 s and 2500 s and are indeed due to deviation from stoichiometry, which in turn comes from non-ideal settling process (overshoot). It is a technicality that can be mitigated by better algorithm tuning, using slower growth rates until the target is reached, using more accurate estimates for starting fluxes, and eliminating the measurements artifacts (abnormally high values of QE_{405nm}/QE_{532nm} in the beginning of the growth are due to slightly photoemissive chamber walls generating additional photocurrent from scattered laser light). QEs in the experiment in Fig. 2 saturate at values that are approximately a factor of 2 lower than expected for Cs_3Sb [6, 9, 11]; an accidental contamination of the Cs source has been confirmed as the cause, the film attains full QE if left in UHV for a few days after the deposition. It is possible that the presence of an undesired contaminant in $Cs_{3+x}Sb$ is distorting the photoemissive properties, namely the value of the QE ratio, as compared to a pure material. We believe that such distortion is not very significant, because our earlier experiments conducted with pure Cs (see, e.g., [12]) are in good agreement with the QE ratio dependence (Fig. 1), in terms of existence of an asymmetric minimum of QE_{405nm}/QE_{532nm} (steep on Cs-rich side, almost flat on Sb-rich side), whose value is not more than 1.7.

To demonstrate the accuracy and robustness of the stoichiometry control, we conducted a variable growth rate experiment, see Fig. 3. Right after the settling of the PID controller on the target of 2.0 for QE_{405nm}/QE_{532nm}, Cs flux was programmed to follow a distinct asymmetric V-shaped pattern vs time. As evident from Fig. 3, the algorithm driving the Sb flux was largely able to keep up with the change of the Cs flux. The ratio of the maximum to minimum flux is about 2.5 for both Cs and Sb based on the calibrations, with the corresponding growth rates between approximately 0.05 and 0.02 Å/s. Note the lag of Sb heater voltage of about 500 s and deviations of the QE_{405nm}/QE_{532nm} from the target value during the process; these are inevitable effects of the algorithm operation. Both effects can be mitigated with better instrumentation and by choosing slower growth rates. Sb heater voltage steps are due to the resolution of the power supply. Dependence of Sb flux on the heater voltage is very non-linear; each voltage step corresponds to approximately 3.7% to 4.0% change of flux. Judging by the amount of the overall distortion of the Sb heater voltage pattern, the accuracy of the stoichiometry control in this experiment can be estimated at a few percent level, also in agreement with the variation of QE_{405nm}/QE_{532nm} between approximately 1.75 and 2.25, see Fig. 1. It is important to note that experiments similar to the one represented by Fig. 3 can serve as a very efficient tool of finding the starting values of flux-setting parameters for fixed growth rate experiments (Fig. 2).

We believe that the principles of the growth scheme demonstrated in this Letter could be immediately applied to some other mono-alkali antimonides, as well as related compounds such as Cs_2Te. Whether or not, and how effectively, the principles can be applied to bi- and multi-alkalis, depends on a particular dependence of photoemissive properties on stoichiometry, now described by more than one parameter. For example, for K_2CsSb a version of dependence in Fig. 1 would become a 3-dimentional plot (surface), where the ratio of QEs is a function of both K and Cs contents (normalized by Sb content). A global minimum likely exists on the surface, whose position is close to the optimum stoichiometry. If there are sufficiently smooth, large, and steep areas around the minimum, then the stoichiometry control can be accomplished using an algorithm that natively supports multiple control parameters [18].

In conclusion, we showed that stoichiometric composition of Cs_3Sb has a strong effect on its photoemissive properties for low temperature growth conditions. We characterized the effect experimentally, by observing the change of QE_{405nm}/QE_{532nm} parameter. Relying on the strong correlation between QE_{405nm}/QE_{532nm} and stoichiometry for slightly Cs-rich films, we developed an automated growth control scheme where one of the fluxes is controlled by an algorithm. Effectively, the scheme maintains QE_{405nm}/QE_{532nm} at a target value around 2 that, in turn, defines a small offset from optimum stoichiometry. Several experiments were conducted with the targets for QE_{405nm}/QE_{532nm} ranging from 1.8 to 3.0; assuming reasonable starting conditions, the scheme always worked. We showed that the scheme is robust and can be used within a wide range of growth rates. Stoichiometry control is a capability that is critical for development of future alkali antimonide growth recipes, such as the ones for MBE. At this point, we do not understand, even qualitatively, physics behind the effect of stoichiometry on photoemissive properties (Fig. 1). We encourage photoemission model developers to explicitly consider the case of slightly non-stoichiometric alkali antimonides; we would be happy to support such efforts by conducting tailored validating experiments and sharing the data.

The authors wish to thank Fangze Liu and Anju Poudel for technical support. VP thanks Dimitre Dimitrov and Enrique Batista for fruitful conversations, and John Lewellen for thorough reading of the manuscript and valuable comments. The authors gratefully acknowledge the support of Los Alamos

PLEASE CITE THIS ARTICLE AS DOI: 10.1063/5.0080948

National Laboratory (LANL) Laboratory Directed Research and Development (LDRD) program, projects 20190536ECR, 20210595DR, and 20220058ER. Los Alamos National Laboratory, an affirmative action equal opportunity employer, is managed by Triad National Security, LLC for the U.S. Department of Energy's NNSA, under contract 89233218CNA000001. This work was also supported by the Office of Science, Office of Basic Energy Sciences of the U.S. Department of Energy under Contract Nos. DE-SC0013190.

DATA AVAILABILITY

The data that support the findings of this study are available from the corresponding author upon reasonable request.

REFERENCES

[1] P. Musumeci, J. Giner Navarro, J.B. Rosenzweig, L. Cultrera, I. Bazarov, J. Maxson, S. Karkare, H. Padmore, Advances in bright electron sources, Nuclear Inst. and Methods in Physics Research, A **907** (2018) 209–220.

[2] Z. Ding, M. Gaowei, J. Sinsheimer, J. Xie, S. Schubert, H. Padmore, E. Muller, and J. Smedley, In-situ synchrotron x-ray characterization of K2CsSb photocathode grown by ternary co-evaporation, Journal of Applied Physics **121**, 055305 (2017)

[3] M. Gaowei, J. Sinsheimer, D. Strom, J. Xie, J. Cen, J. Walsh, E. Muller, and J. Smedley, Codeposition of ultrasmooth and high quantum efficiency cesium telluride photocathodes, Phys. Rev. Accel. Beams **22**, 073401 (2019)

[4] Alice Galdi, Jan Balajka, William J. I. DeBenedetti, Luca Cultrera, Ivan V. Bazarov, Melissa A. Hines, and Jared M. Maxson, Reduction of surface roughness emittance of Cs3Sb photocathodes grown via codeposition on single crystal substrates, Appl. Phys. Lett. **118**, 244101 (2021).

[5] G. Gevorkyan, S. Karkare, S. Emamian, I. V. Bazarov, and H. A. Padmore, "Effects of physical and chemical surface roughness on the brightness of electron beams from photocathodes", Phys. Rev. Accel. Beams **21** (2018) 093401

[6] A. Sommer, "Photoemissive materials. Preperation, properties and uses." Huntington: Krieger, 1980.

[7] K. H. Jack and M. M. Wachtel, The Characterization and Crystal Structure of Caesium Antimonide, a Photo-Electric Surface Material, Proceedings of the Royal Society of London. Series A, Mathematical and Physical Sciences, Vol. 239, No. 1216 (Feb. 12, 1957), pp. 46-60.

[8] Clayton W. Bates, Jr., Dhruba Das Gupta, Luis Galan, D.N.E. Buchanan, X-ray photoemission studies of cesium antimonide photoemitters, Thin Solid Films, **69** (1980) 175-182.

[9] Luca Cultrera, Ivan Bazarov, Adam Bartnik, Bruce Dunham, Siddharth Karkare, Richard Merluzzi, and Matthew Nichols, Thermal emittance and response time of a cesium antimonide photocathode, Appl. Phys. Lett. **99**, 152110 (2011)

[10] Jun Feng, Siddharth Karkare, James Nasiatka, Susanne Schubert, John Smedley, and Howard Padmore, Near atomically smooth alkali antimonide photocathode thin films, Journal of Applied Physics **121**, 044904 (2017).

[11] L. Cultrera, S. Karkare, H. Lee, X. Liu, I. Bazarov, and B. Dunham, “Cold electron beams from cryocooled, alkalai antimonide photocathodes,” Physical Review Accelerators and Beams, **18**, 133401 (2015).

[12] V. Pavlenko, A. Scheinker, M. A. Hoffbauer, F. Liu, and N. A. Moody, Towards adaptive, automated growth of photocathodes, Photocathode Physics for Photoinjectors (P3) Workshop, Santa Fe, NM, 2018.

[13] Alice Galdi, William J. I. DeBenedetti, Jan Balajka, Luca Cultrera, Ivan V. Bazarov, Jared M. Maxson, and Melissa A. Hines, The effects of oxygen-induced phase segregation on the interfacial electronic structure and quantum efficiency of Cs3Sb photocathodes, J. Chem. Phys. **153**, 144705 (2020).

[14] H. Panuganti, E. Chevallay, V. Fedosseev, M. Himmerlich, Synthesis, surface chemical analysis, lifetime studies and degradation mechanisms of Cs-K-Sb photocathodes, Nuclear Inst. and Methods in Physics Research, A **986** (2021) 164724.

[15] A. Alexander, M. Gaowei, S. Mistry, J. Walsh, F. Liu, K. Evans-Lutterodt, E. Stavitski, V. Pavlenko, J. Smedley, and N. Moody, Robust method for broadband efficiency enhancement of electron photocathodes using optical interferences, AIP Advances **11**, 065325 (2021)

[16] Mark Hoffbauer, Vitaly Pavlenko, John Lewellen, and Nathan Moody, The ACERT Multiphysics Photocathode Growth and Characterization System, Photocathode Physics for Photoinjectors (P3) Workshop, Newport News, VA, 2016.

[17] Accurate measurement and calibration of the substrate temperature is a complicated issue, particularly in the range of interest, <200°C. Because of the significance of the parameter for thin film growth, the issue needs to be addressed systematically in the future studies in order to minimize ambiguities and discrepancies between reported values.

[18] Scheinker, A. and Scheinker, D., Bounded extremum seeking with discontinuous dithers. Automatica, **69**, 250-257 (2016), https://doi.org/10.1016/j.automatica.2016.02.023

FIGURE 1

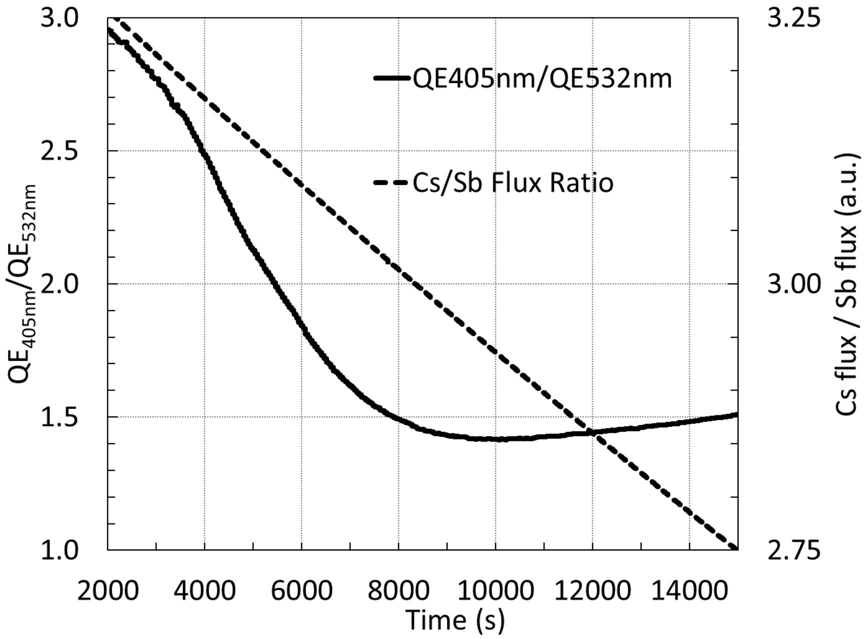

Figure 1 Response of Cs_3Sb film photoemission to a gradual change of incident fluxes ratio.

FIGURE 2

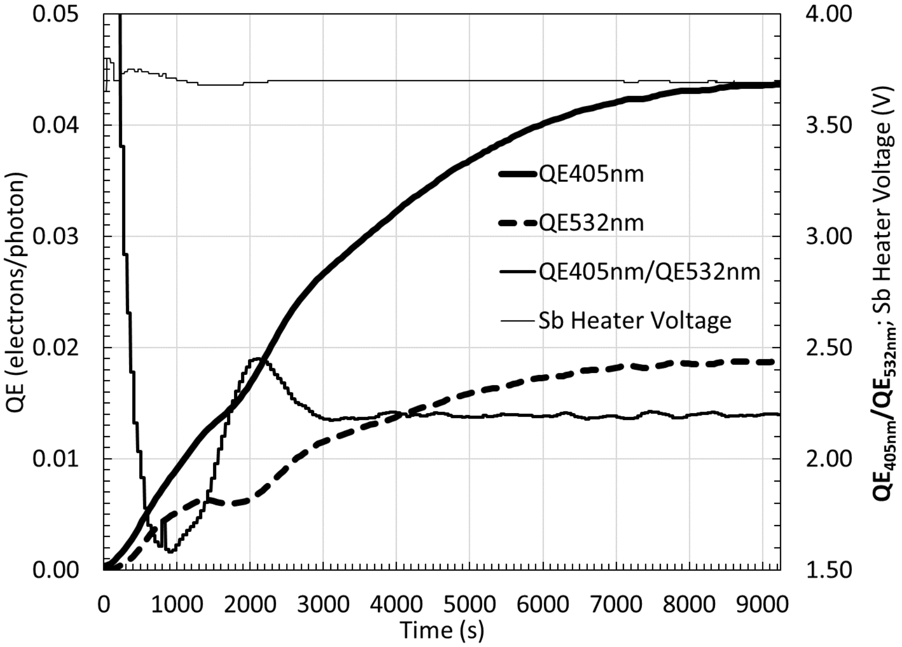

Figure 2 Algorithm-controlled growth of Cs_3Sb film. Cs flux is kept approximately constant. Target for QE_{405nm}/QE_{532nm} is set at 2.2.

FIGURE 3

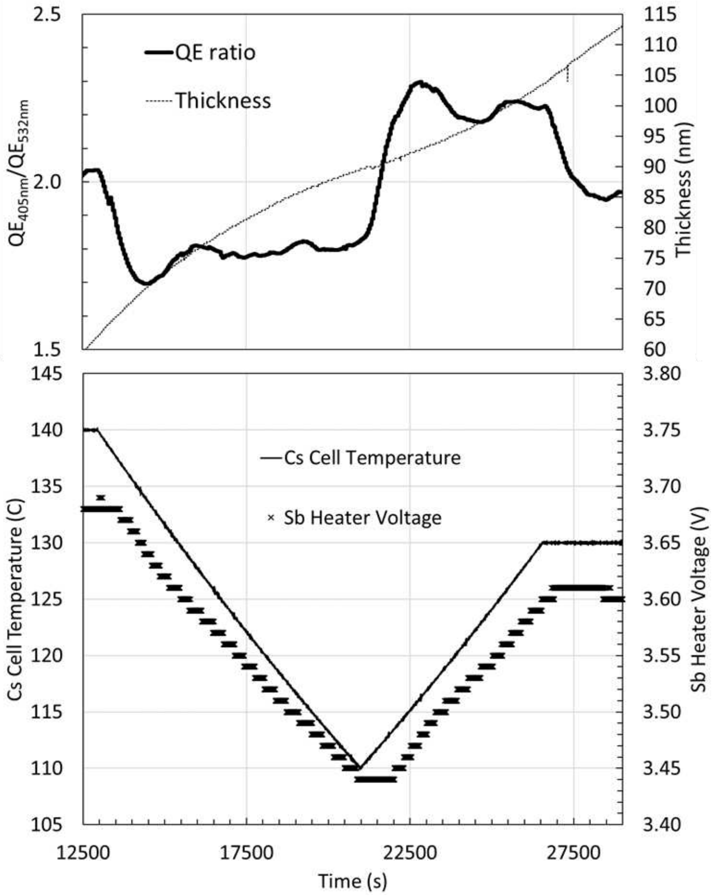

Figure 3 Variable growth rate experiment. Sb flux is controlled by PID loop. Target for QE_{405nm}/QE_{532nm} is set at 2.0. Thickness is approximate, estimated with a quartz crystal microbalance. See text for details.

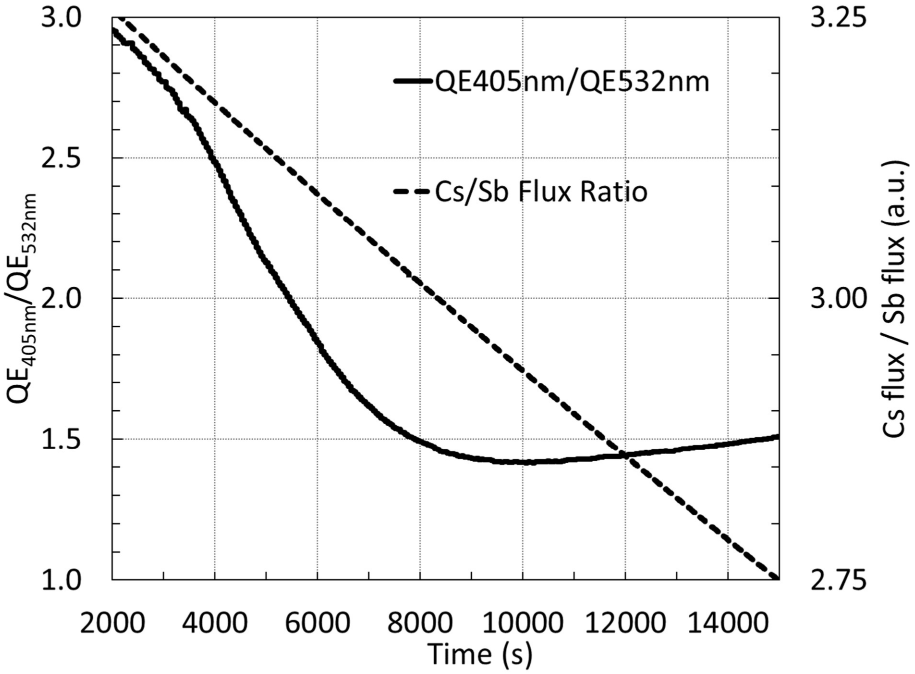
QE405nm/QE532nm
Cs/Sb Flux Ratio
QE_{405nm}/QE_{532nm}
Cs flux / Sb flux (a.u.)
Time (s)
3.0
2.5
2.0
1.5
1.0
3.25
3.00
2.75
2000
4000
6000
8000
10000
12000
14000

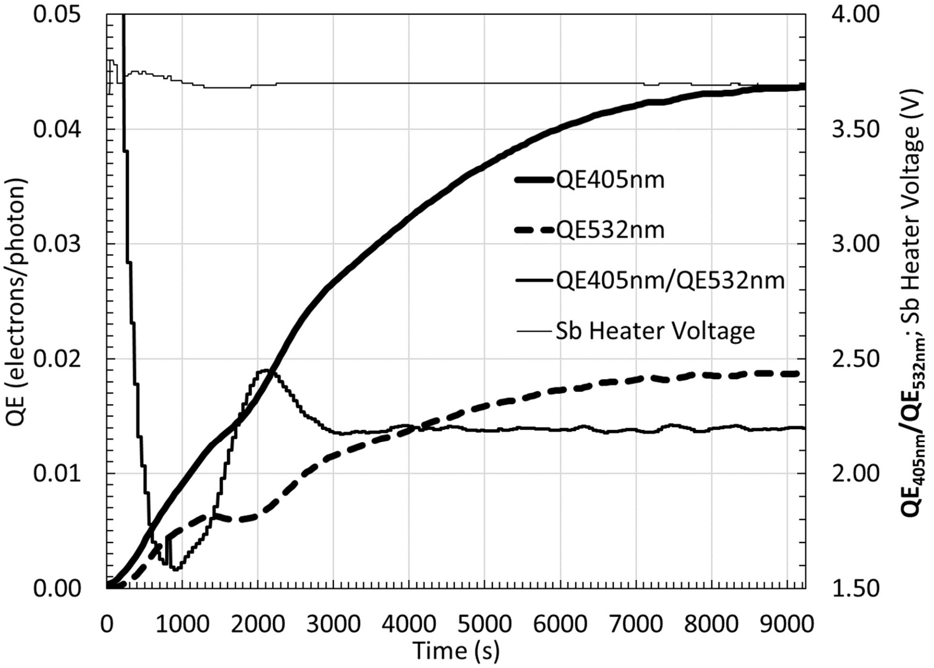
QE (electrons/photon)
0.05
0.04
0.03
0.02
0.01
0.00
0
1000
2000
3000
4000
5000
6000
7000
8000
9000
Time (s)
4.00
3.50
3.00
2.50
2.00
1.50
QE_{405nm}/QE_{532nm}; Sb Heater Voltage (V)
QE405nm
QE532nm
QE405nm/QE532nm
Sb Heater Voltage

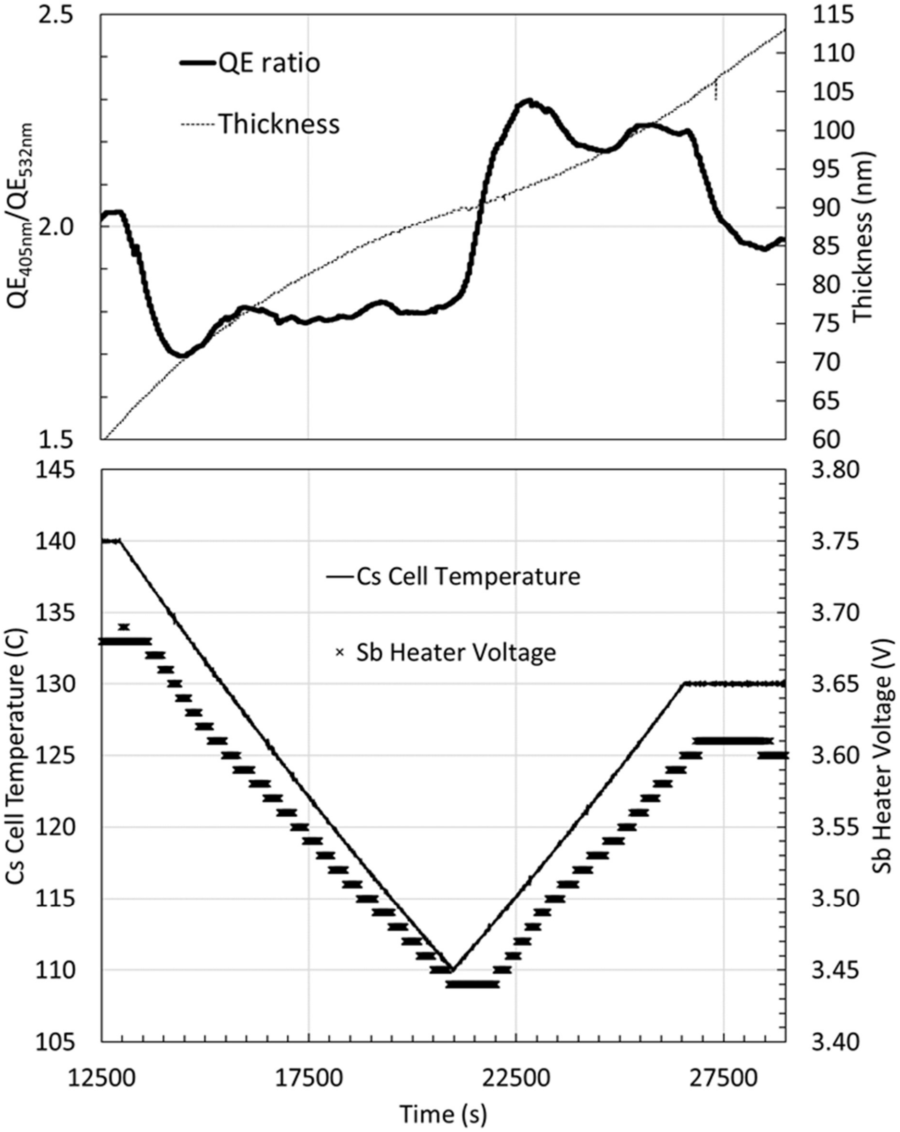
QE ratio
Thickness
QE_{405nm}/QE_{532nm}
Thickness (nm)
2.5
2.0
1.5
115
110
105
100
95
90
85
80
75
70
65
60
Cs Cell Temperature
× Sb Heater Voltage
Cs Cell Temperature (C)
Sb Heater Voltage (V)
145
140
135
130
125
120
115
110
105
3.80
3.75
3.70
3.65
3.60
3.55
3.50
3.45
3.40
12500
17500
22500
27500
Time (s)